Quantitative Studies of Endothelial Cell Adhesion

Directional Remodeling of Focal Adhesion Sites in Response to Flow Forces

Peter F. Davies,* Andre Robotewskyj,* and Melvin L. Griem[‡]
Departments of *Pathology and ‡Radiation and Cellular Oncology, Pritzker School of Medicine,
The University of Chicago, Chicago, Illinois 60637

Abstract

Focal adhesion sites were observed in cultured endothelial cells by tandem scanning confocal microscopy and digitized image analysis, techniques that provide real-time images of adhesion site area and topography in living cells. Image subtraction demonstrated that in the presence of unidirectional steady laminar flow (shear stress $[\tau] = 10$ dyn/cm^2) a substantial fraction of focal adhesion sites remodeled in the direction of flow. In contrast, focal adhesions of control (no flow) cells remodeled without preferred direction. In confluent monolayers subjected to shear stresses of 10 dyn/cm^2, cells began to realign in the direction of flow after 7–9 h. This was accompanied by redistribution of intracellular stress fibers, alignment of individual focal adhesion sites, and the coalescence of smaller sites resulting in fewer, but larger, focal adhesions per cell. Cell adhesion, repeatedly calculated in the same cells as a function of the areas of focal contact and the separation distances between membrane and substratum, varied by < 10% during both short (30 min), or prolonged ($\leq$ 24 h), periods of exposure to flow. Consistent with these measurements, the gains and losses of focal adhesion area as each site remodeled were approximately equivalent. When the glass substratum was coated with gelatin, rates of remodeling were inhibited by 47% during flow ($\tau = 10$ dyn/cm^2). These studies: (a) reveal the dynamic nature of focal adhesions; (b) demonstrate that these sites at the ablumenal endothelial membrane are both acutely and chronically responsive to frictional shear stress forces applied to the opposite (lumenal) cell surface; and (c) suggest that components of the focal adhesion complex may be mechanically responsive elements coupled to the cytoskeleton. (*J. Clin. Invest.* 1994. 93:2031–2038.) Key words: shear stress • cytoskeleton • integrins • mechanotransduction • hemodynamics

Introduction

Endothelial cells, like all anchorage-dependent cells, adhere to the extracellular matrix at focal adhesions, specialized regions of the cell surface where the cell membrane approaches to

within 15 nm of the substratum (1–4). These anchorage sites play a critical role in the maintenance of cell shape, differentiated properties, and the control of cell proliferation and migration (3). The direct observation of focal adhesion sites in living endothelial cells in real time by tandem scanning confocal microscopy (5) combined with quantitative image analysis has recently provided topographical estimates and measurements of the dynamic properties of these specialized membrane regions (6). Most sites undergo continuous remodeling of the separation distances between the ablumenal cell surface and the substratum. Remodeling in undisturbed endothelial cells appears random in direction and varies in magnitude between individual adhesion sites in the same cell. Focal adhesions help maintain cell shape by anchoring actin filaments that, together with other cytoskeletal components, distribute tension throughout the cell. The microfilaments associate with specific integral membrane proteins (primarily integrin $\alpha_v\beta_3$ in endothelial cells) that span the plasma membrane and bind to extracellular adhesion proteins (3, 7–9). The actin-integrin association appears to be indirect, mediated via linker proteins such as α-actinin, talin, and vinculin (3, 10), although the precise molecular interactions within the complex are poorly understood. The cytoskeletal network also interacts with other membrane sites, including junctional proteins between cells, integrins and receptors on the endothelial lumenal surface, and nuclear membrane proteins (11–15). There is therefore a complex network of tension-bearing elements that provides a mechanical continuum throughout the cell extending across the plasma membrane to the extracellular matrix. The interplay between cytoskeletal tension and integrin association with extracellular adhesion proteins has been shown to be important in the regulation of cellular structure and function (13, 16–18).

Many studies have demonstrated that hemodynamic forces, particularly shear stress, induce a variety of acute and chronic changes of arterial structure and function (reviewed in references 15 and 19). Endothelial cells located at the interface between blood and vessel wall represent a signal transduction system for flow forces acting upon the vessel wall. The location of mechanotransduction elements in endothelial cells is unknown; some kind of flow "sensor" at the lumenal cell surface where frictional shear stresses first interact with the cell is a logical candidate. However, the continuum of structures between the lumenal plasma membrane and the subcellular extracellular matrix is continuously under tension in adherent cells (13). The anchoring of cytoskeletal elements at focal adhesions suggests that these regions may be flow responsive. Here we demonstrate that endothelial focal adhesion sites observed in real time are directionally responsive to hemodynamic shear stress forces imposed on the cell, and we speculate that these sites may be involved in the cascade of electrophysiological (20), biochemical (21), and gene regulatory (22) responses that result when endothelium is exposed to flow.
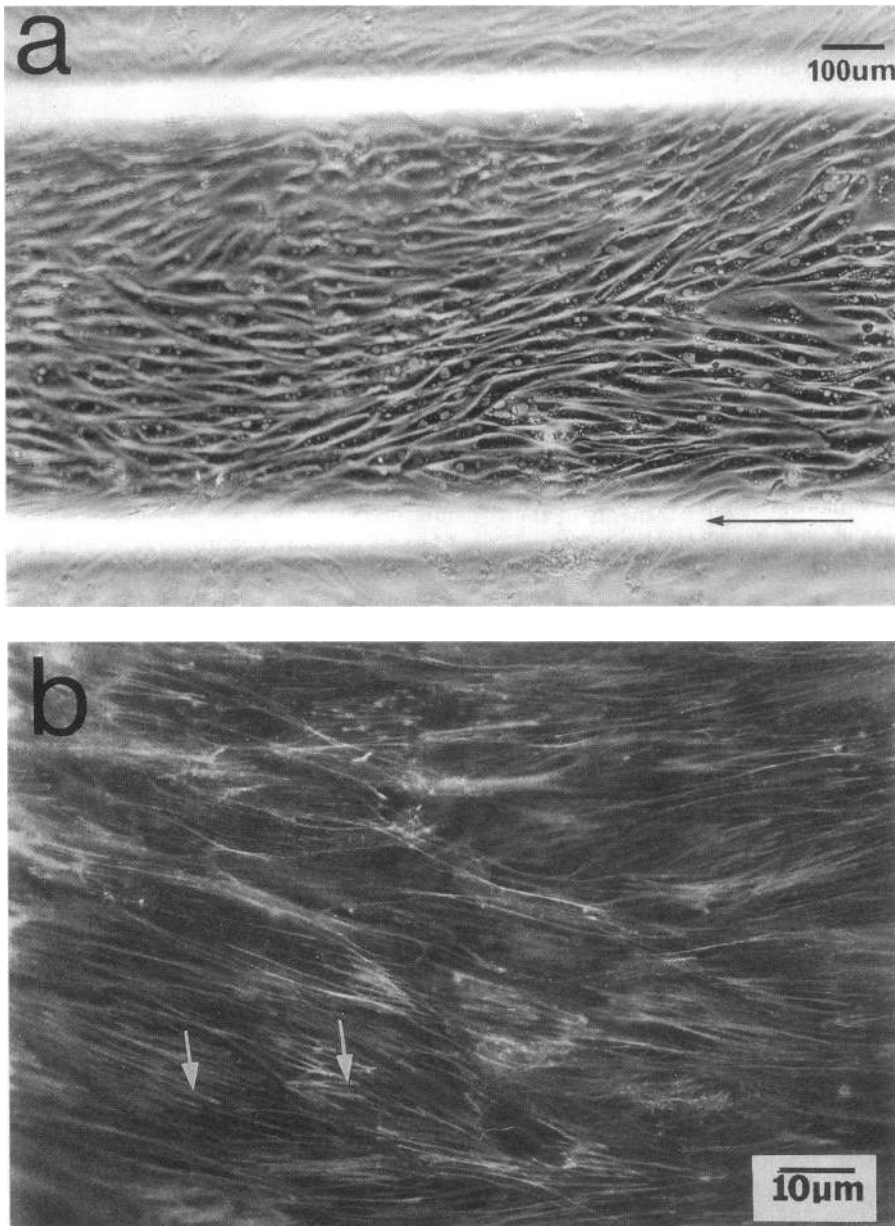
Figure 1. (*a*) Low-power phase contrast micrograph of confluent bovine aortic endothelial cells after alignment in a capillary flow tube (1-mm width). 10 dyn/cm² shear stress in laminar flow for 48 h. (*b*) F-actin stress fiber distribution in aligned, confluent endothelial cells (NBD-phallacidin stain). Longer arrow shows flow direction for both *a* and *b*.

Methods

Cell culture. Bovine aortic endothelial cells (BAEC)[1] were isolated and cultured by standard procedures (23) and used between passages 7 and 20. In all experiments the cells were grown in small-diameter flow tubes as previously described (20). After trypsinization, a cell suspension was plated at subconfluent density into 1 × 1-mm-square cross-section borosilicate glass capillary flow tubes (24) (Vitro Dynamics, Rockaway, NJ) that were untreated or in some experiments precoated with 0.1% gelatin. The thickness of the gelatin layer, a contributor to the cell–glass separation distance, was measured as 6±1 nm by atomic force microscopy (K. Barbee, R. Lal, and P. F. Davies; unpublished results). BAEC were bathed in DME (high glucose; GIBCO BRL, Gaithersburg, MD) containing 10 mM N-2-hydroxyethylpiperazine-N^1-2-ethane sulfonic acid (Hepes), 2 mmol/ml glutamine, 100 U/ml penicillin, 100 μg/ml

---

1. *Abbreviations used in this paper:* BAEC, bovine aortic endothelial cells; FFT, fast fourier transform; TSCM, tandem scanning confocal microscope.

streptomycin, and 10% heat-inactivated calf serum (GIBCO BRL). After the cells had plated on one wall of the tube, all subsequent routine medium changes were conducted by capillary exchange. All images were obtained within 48 h after the cells reached confluence.

Confocal microscopy. Phase contrast and confocal images were viewed using a tandem scanning confocal microscope (TSCM; Noran, Madison, WI) equipped with long working distance Planapo 40× and Neofluar 100× oil immersion lenses with high numerical apertures (1.0 and 1.25, respectively; Carl Zeis, Inc., Thornwood, NY) to concentrate the available light (xenon source) and to provide images constituted from zero-order interferences as previously described (6). Cells were observed from outside of the capillary tube. To maintain pH and facilitate nutrient supply and waste removal in the tubes, three tube-volume changes per minute were maintained by slow perfusion (150 μl/min) using a closed flow circuit driven by a peristaltic pump (Harvard Apparatus, S. Natick, MA) with appropriate pulse dampening, pH, and temperature control systems. The optical plane of the TSCM (0.7-μm thickness) was positioned just below the cell and raised until it overlapped the interface between the cell and substratum. Images from the TSCM were directed via an intensified CCD video camera (Video-

scope International, Washington, DC) and relay lens to produce an analogue video signal that was digitized and converted to 640 × 480 pixels by an image analysis system (QX-7 214; Quantex Corp., Sunnyvale, CA). To minimize alterations in cell behavior resulting from long periods of exposure to high illumination intensity in the visible range (400–700 nm) (25), illumination was blocked between measurement periods. A typical interval of exposure for image acquisition was 20 s. Images were collected in real time, averaged to reduce noise and increase sharpness, and corrected for uneven illumination. Image analyses of adhesion sites were conducted by radiance analysis procedures that measured the area of each adhesion site, its radiance, and location using image recording and analysis software routines (Quantex Corp.). Cell adhesion was calculated from area and radiance measurements as described previously (6). Focal contacts were identified by the large decrease in radiance level associated with them; this allowed elimination of other image detail by gray level thresholding. The limits of resolution for detection of focal contacts using ×100 objective was 2 × 10^{-2} μm^2 of cell membrane. Further processing of images was conducted on Macintosh IIfx and Centris 650 computers (Apple Computer, Copertino, CA). Spatial estimates between the cell and substratum at adhesion sites (i.e., topography of adhesion) were made as described previously (6), in which radiance values were plotted against separation distance calibrated for zero order to first order interference patterns. A minimum separation distance was set at 15 nm. The calibration curve obtained from the living cell was linearized by transformation and stored in computer memory for referencing radiance/separation distances within the same cell as well as in other cells in the same field. A program was written to automatically calculate the separation distance when a cursor was positioned over different parts of the cell.

Flow loop. Insertion of the capillary flow tubes into a recirculating flow loop permitted control of the perfusion rate (and shear stress). Components of the loop were connected by small-bore silastic tubing (Cole Parmer, Chicago, IL). A reservoir of culture medium (250 ml) was maintained at 37°C adjacent to the microscope stage, which was enclosed by a temperature-regulated Plexiglass incubator. Medium, gently gassed with air/5% CO$_2$, was drawn through the system by a flow pump (Harvard Apparatus). To dampen pulsatility, the main reservoir was vented and two buffer reservoirs were inserted between the pump and flow tube. Tracer microbubbles injected into the loop flowed over the cells at constant velocity. Wall shear stress was calculated for a circular cross sectional tube as a function of flow velocity, medium viscosity (0.77 centipoise), and tube geometry as previously outlined (20). This calculation is valid at the midpoint of the tube but slightly overestimates shear stresses with increasing distance from the midpoint. Cell images were therefore obtained in the monolayer at or within 100 μm of the midpoint of the tube. At the extreme positions at which images were acquired, the shear stress was 9.6 dyn/cm^2 (vs. 10.0 dyn/cm^2 at the midpoint).

Fluorescence staining. Cells were fixed with 4% formaldehyde in PBS for 20 min at 37°C. After three washes with PBS, the cells were permeabilized by 0.1% Triton X-100 in PBS for 3 min at room temperature, washed twice with PBS, then three times with 50 mM ammonium chloride, pH 7.3, for 5 min each wash. Filamentous actin (F-actin) was stained by addition of N-(nitrobenz-2-oxa-1,3-diazol-4-yl)-phallacidin (Molecular Probes, Inc., Eugene, OR) at a dilution in PBS of 1:100 of a 3-mM stock solution, for 20 min at room temperature followed by three final washes in PBS. After infusion of glycerol/PBS (1:10; containing 2 mg/ml p-phenyldiamine) into the capillary tubes, cells were viewed using a fluorescence microscopy (E. Leitz Inc., Rockleigh, NJ) equipped with epifluorescence using narrow band pass excitation and emission filters for fluorescein and rhodamine (Omega Optical Company, Burlington, VT).

Image acquisition. Additional photomicrographs were obtained using an inverted microscope (IMT-2; Olympus, Lake Success, NY) in phase contrast mode. Cell images were photographed on 35-mm Kodak T-Max film, ASA 400, or Fuji ASA 3200 film, by directing the light path to a camera (OM-4; Olympus), attached to either the TSCM or the Olympus inverted microscope, or a Leitz photomicrographic sys-

tem (Leitz vario orthomat; X40/0.9NA, X100/1.1NA lenses) for nonconfocal fluorescence image recording. Digitized, processed confocal images were routed directly to a color printer. Fast fourier transform (FFT) analyses of images obtained after intervals of exposure to directional shear stress were performed using a FFT analytical package (Systat, Evanston, IL).

Results

All data were obtained from endothelial cells in a confluent monolayer. During acute exposure to flow there was no significant repositioning of the cell boundaries. During extended periods of flow the shape of individual cells remodeled but the overall position of each cell did not. Thus focal adhesion remodeling was observed and cell adhesion was quantitated in the absence of cell migration or cell positional changes within the monolayer.

When confluent bovine aortic endothelial cells were subjected to unidirectional laminar flow (shear stress [τ], 10 dyn/cm^2), cells became elongated and aligned in the direction of flow over a period of 24–48 h (Fig. 1 a). During the same interval, the filamentous actin cytoskeleton reorganized into parallel arrays of elongated stress fibers that also aligned in the
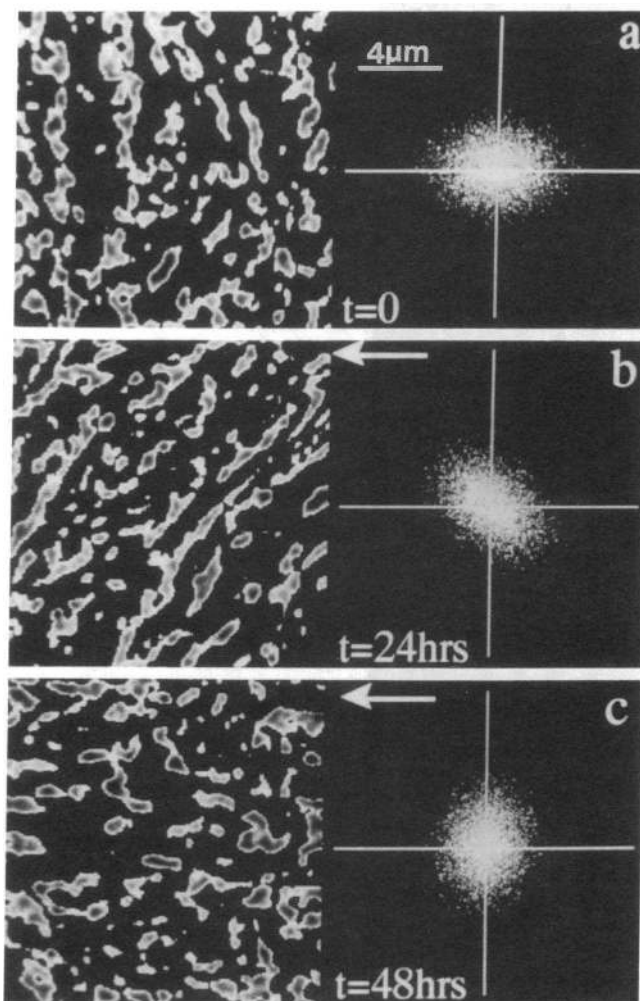

Figure 2. Reorganization of focal adhesion morphology in confluent endothelial cells during prolonged flow at times (a) 0, (b) 24, and (c) 48 h. (*Left*) Processed TSCM images of focal contact regions. (*Right*) Corresponding FFT patterns that demonstrate progressive realignment. 10 dyn/cm^2 shear stress in direction of arrow.

direction of flow (Fig. 1 b). Prominent stress fibers terminate within the cell at focal adhesion sites and at the junctions between adjacent cells of the confluent monolayer (6, 11, 12).

Sites of focal contact between the ablumenal cell surface and glass substratum occur throughout the endothelial cell. In the TSCM, focal adhesions were identified as regions of substantially decreased radiance levels that permit their optical isolation from other cellular detail by gray level thresholding. The differential radiance values occur because of refractive index differences of the cell membrane, the glass, and the fluid between them as described previously (6). After processing the digitized image, regions of plasma membrane closer than 50 nm from the substratum were retained; other cell information was removed from the image. The distance of least separation was estimated to be 10–15 nm (1–4, 6, 26). TSCM images of confluent living cells in the flow field (10 dyn/cm^2) revealed a progressive alignment of focal adhesion sites parallel to the flow direction (Fig. 2, a–c), a change confirmed by FFT patterns of the distribution of focal adhesion orientation in the field of confluent cells at intervals of 24 and 48 h (Fig. 2). FFT

data shown in Fig. 2 were obtained from the corresponding focal adhesion images in the adjoining panels.

Repetitive measurements of individual focal adhesions at shorter intervals during the remodeling process frequently revealed the coalescence of multiple sites to form larger areas of membrane attachment elongated in the direction of flow (Fig. 3). The rearrangements occurred rapidly (several minutes) and resulted in a reduction of the number of focal adhesion sites per cell; however, there was little change in the total area of focal contact with the substratum (see below). Such responses to flow were nonuniform; focal adhesions adjacent to those undergoing alignment often showed minimal change as is apparent in the image sequence of Fig. 3.

We have recently demonstrated the dynamic properties of endothelial focal adhesions in undisturbed cells (6). The boundaries of individual focal adhesions extended and diminished in an apparent random fashion over periods of several minutes without any dominant orientation associated with the remodeling. Fig. 4 demonstrates the changes in focal adhesion sites within a small area of endothelial membrane after a period of 15 min at control (no flow) values of shear stress during which the tube was perfused at a rate of three tube changes/min ($\tau = 0.029$ dyn/cm^2). Two images 15 min apart were subtracted to reveal additional areas of focal contact (brown), unchanged location (blue), and area that had disappeared or moved (yellow) during the interval between acquisition of the images. In contrast, the focal contact sites of cells exposed to unidirectional shear stress of 10 dyn/cm^2 showed significant
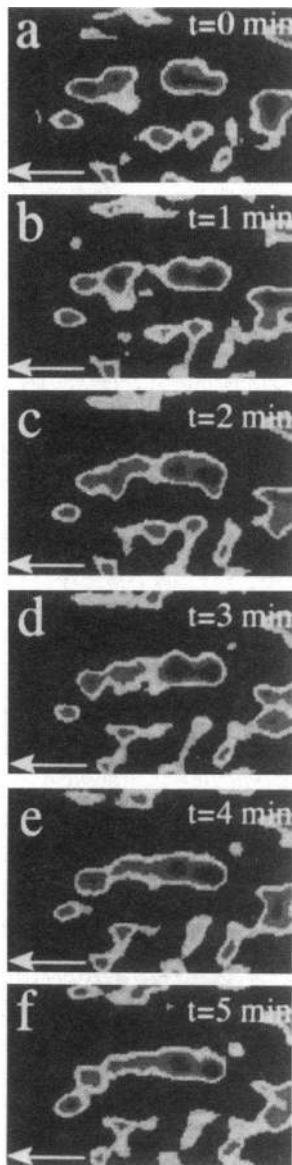
Figure 3. Detailed real time images 1 min apart of reorganizing focal contact regions in a cell within a confluent monolayer during flow. Progressive fusion and alignment of regions occurred over a short interval. Note that the small area to the left of the newly forming aligned site did not significantly change, whereas other sites, above and below, migrated in the direction of flow (arrow). Each panel is 4 × 3 µm.
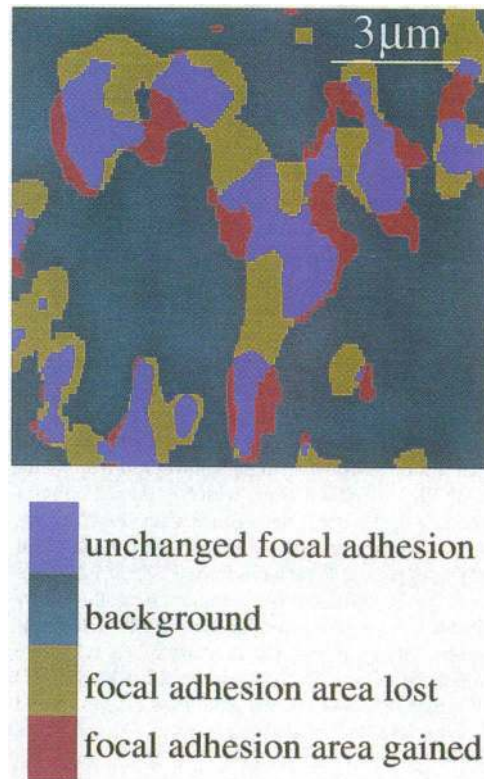
Figure 4. Two-dimensional representation of the remodeling of focal contact sites in part of a control cell (no-flow) within a confluent monolayer during a 15-min interval. Changed and unchanged areas were identified by image subtractions. The orientation of remodeling was random.
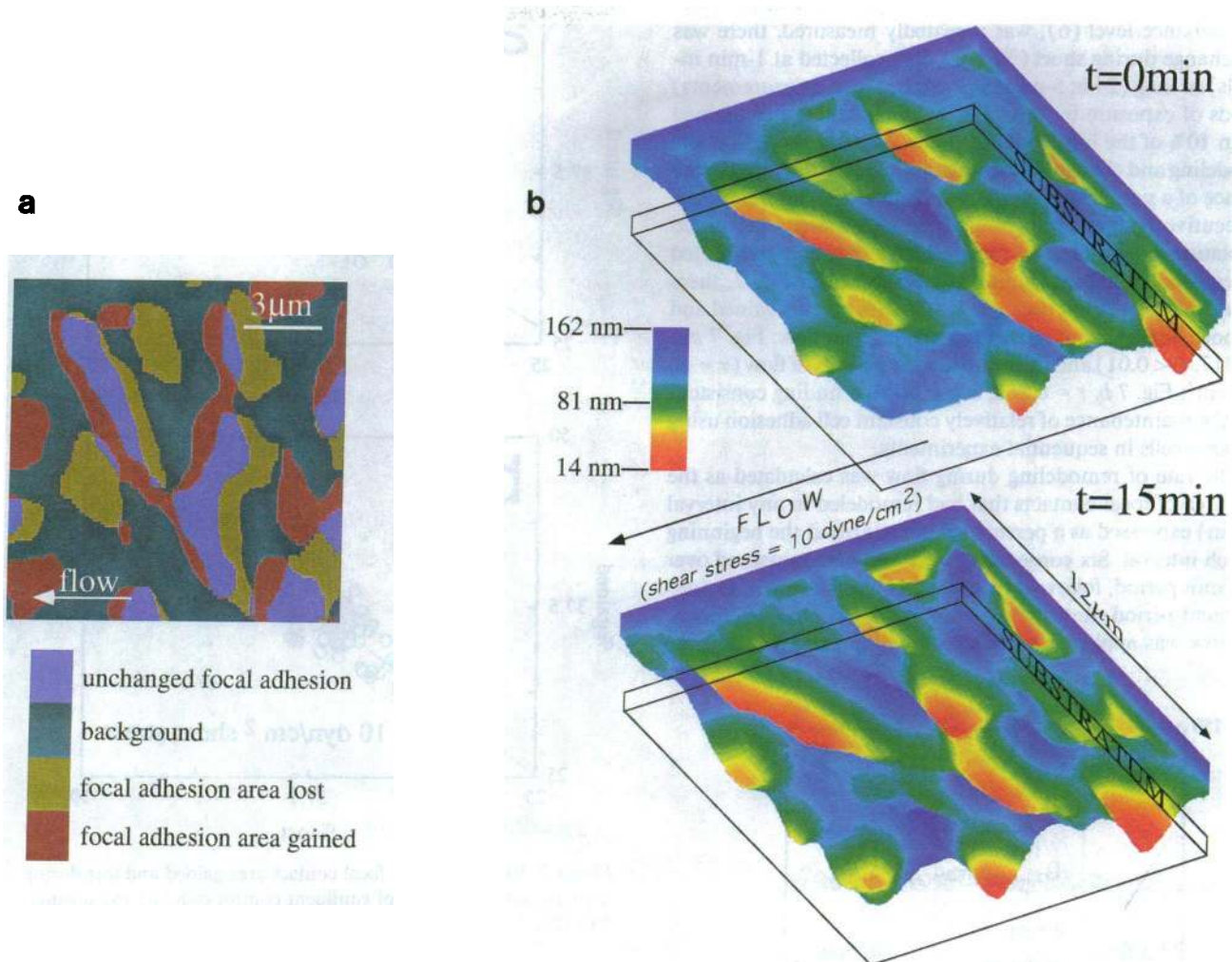
Figure 5. Directional remodeling of focal contact areas during a 15-min interval in part of a cell within a confluent monolayer subjected to flow (10 dyn/cm² shear stress). Remodeling occurred preferentially in the direction of flow (downstream gain/upstream loss of contact). (*a*) Two-dimensional representation obtained from subtraction of processed images. (*b*) Three-dimensional topography of the same cell region (12 × 12-μm membrane) in close and focal contact with the substratum. The spatial relationships of the ablumenal cell membrane with the glass surface are viewed from below the glass. Separation distances between membrane and substratum are shown as a color scale in which the closest interactions at focal adhesions are red. Calibration of separation distance was as previously described (6). At the end of the flow interval most sites have remodeled in the direction of flow (as shown more clearly in Fig. 7 *a*). Of particular note, however, is that separation distances at several sites have changed, reflecting altered cell surface interactions.

remodeling in the direction of flow during a similar interval (Fig. 5 *a*). Although most focal adhesion sites remodeled directionally, some underwent minimal change. Furthermore, the timing of the responses varied; in some cells, directional remodeling occurred coincident with the onset of flow, whereas in other cells it was delayed. The three-dimensional (3D) topography of a portion of ablumenal cell membrane that has been color calibrated with estimates of separation distances between cell and substratum (6) is shown in Fig. 5 *b* after a 15-min time interval. Substantial directional remodeling of focal contact sites occurred in response to flow such that the focal contact sites were repositioned slightly downstream from the origin. Separation distances also changed slightly during directional remodeling as reflected by altered color intensities. The cell boundaries within the confluent monolayer were unchanged during this interval, and uniform "treadmilling" of the ablumenal membrane was contraindicated by the nonresponsiveness of several adjacent focal contact sites. Although shifts in

the location of focal contact sites can be appreciated more readily in the 2-D subtraction images, such as Fig. 5 *a*, the 3-D topographic plots (Fig. 5 *b*) provide additional valuable information about the changing relationship between cell membrane and substratum during remodeling. The elements of focal adhesion area and separation distance (determined from radiance) were combined to estimate relative values for cell adhesion in real time.

Cell adhesion is related to some function of the area of ablumenal plasma membrane in close contact with the substratum and, within such areas, may be further influenced by the intimacy of contact between the cell and the extracellular matrix, i.e., separation distance. A focal adhesion site is defined by a sharp decline in radiance level compared with that of cell membrane that is immediately adjacent. Within each focal adhesion site, a narrow range of radiance values was measured. Together, these characteristics suggest that the area and closeness of contact are principal determinants of adhesion (26).

When cell adhesion, defined as focal adhesion area times reciprocal radiance level (6), was repeatedly measured, there was little change during short (30 min; data collected at 1-min intervals) or long (24 h; 5-min intervals between measurements) periods of exposure to flow (Fig. 6). Cell adhesion remained within 10% of the initial values. Thus, extensive adhesion site remodeling and change of alignment of the cells occurred in the absence of a significant change of cell adhesion. Subtraction of consecutive images throughout these experiments permitted calculation of the area of focal contact that had remodeled between individual measurements. As shown in Fig. 7, there was a close correlation between focal adhesion area gained and lost both during spontaneous remodeling (no flow; Fig. 7 a; r = 0.817, P < 0.01) and during extended periods of flow (τ = 10 dyn/cm²; Fig. 7 b; r = 0.862, P < 0.005), a finding consistent with the maintenance of relatively constant cell adhesion using the same cells in sequential experiments.

The rate of remodeling during flow was calculated as the total area of focal contacts that had remodeled in any interval (5 min) expressed as a percentage of the area at the beginning of each interval. Six consecutive intervals were measured over a 30-min period, followed by a 1-h delay before the next measurement period. Rates of remodeling were similar whether or not flow was applied when cells were compared on the same
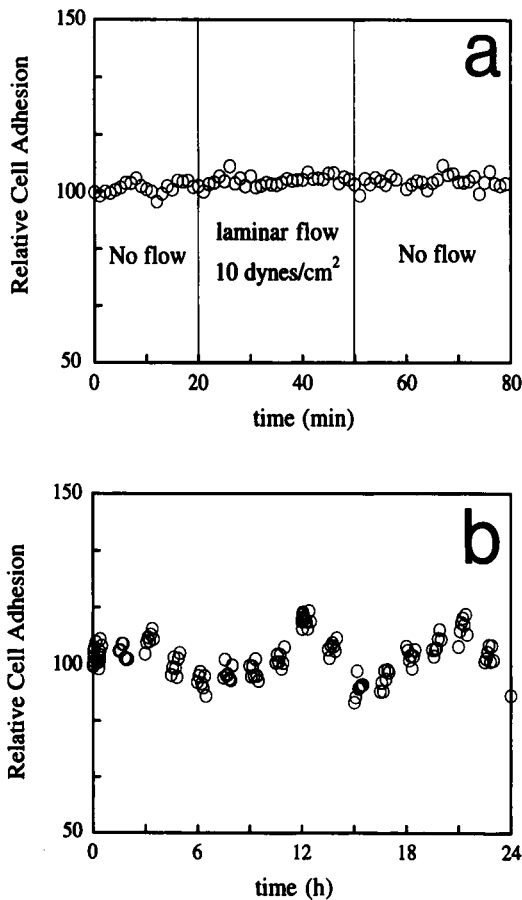

Figure 7. Relationship of focal contact area gained and lost during spontaneous remodeling of confluent control cells (*a*) and during flow (*b*).

Figure 6. Cell adhesion in confluent endothelial cells subjected to short (30 min, *a*) and long (24 h, *b*) periods of exposure to flow. Images were acquired from regions equivalent to one to two cells at 1-min intervals (*a*) or several times each hour (*b*). Cell adhesion was calculated from focal contact area and radiance measurements as previously described (6).
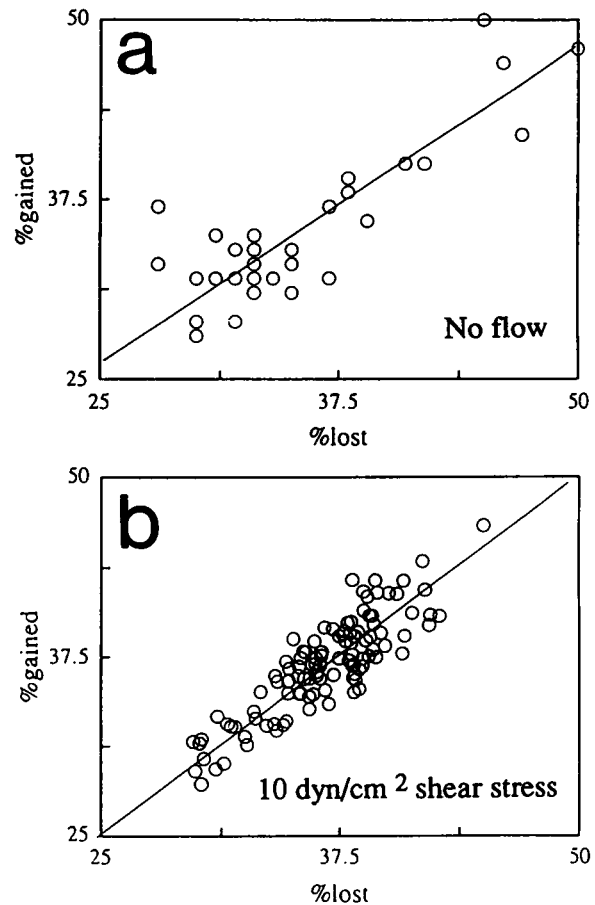
substratum. However, as shown in Fig. 8, there was a significant difference in focal adhesion dynamics when the substratum was changed. When a 6-nm film of gelatin was precoated over the interior of the flow tube, the remodeling rate in confluent endothelial cells decreased from a mean of 35.3±2.6 area units to 18.8±1.8 (Fig. 8 b), a decrease of 46.7% (P < 0.005) compared with the "untreated" surface throughout an 18-h period of flow (Fig. 8 a). Realignment of cells during flow was not inhibited by gelatin. In similar experiments (not shown) but of shorter duration (8 h) and using control (no-flow) confluent cells, gelatin also inhibited the remodeling process (mean inhibition, 51.8%±7.4; P < 0.005). These observations suggest that the dynamics of focal adhesion site interactions with the substratum are matrix regulated.

Images that had been processed for focal adhesion enhancement in the Quantex system were subsequently observed as a movie sequence using the Apple Quicktime facility to attempt to detect spatial and temporal patterns of focal adhesion redistribution during flow. Coordinated bursts of focal adhesion remodeling were observed at irregular intervals during flow with major reorientation of the sites in the direction of flow commencing after 5 h. However, there were no predictable regions of the cell where reorganization was prevalent nor were the periods of reorganization of equal length. In control (no flow) cells, irregular bursts of focal adhesion remodeling were also noted but the changes were not directional.
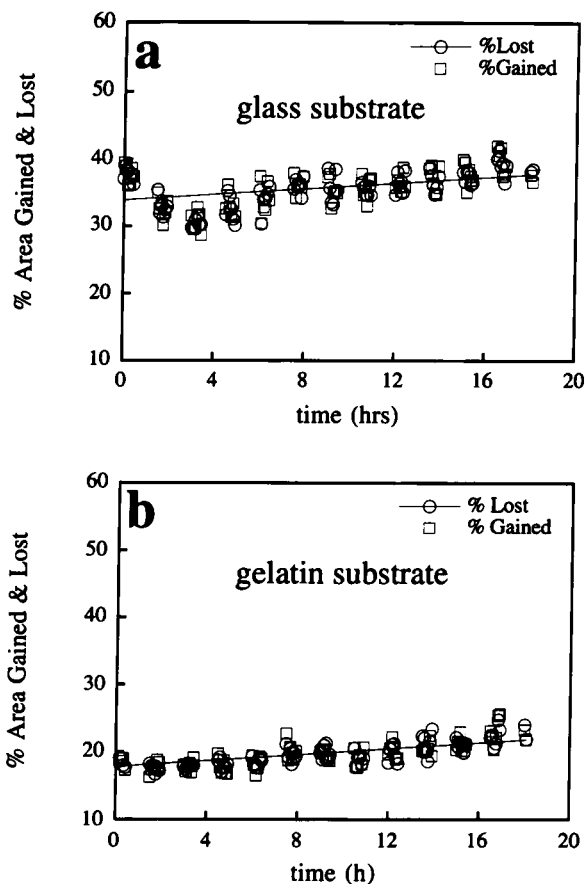
Figure 8. Rates of remodeling of areas of focal contact in confluent endothelial cells during (*a*) flow-directed remodeling of cells grown on glass, and (*b*) flow-directed remodeling on gelatin. The area gained and lost was expressed as a percent of the total area of focal contact at the beginning of the measuring interval (5 min). Each measuring period of six consecutive measurements (30 min) was followed by a gap of 1 h when no data were gathered.

Discussion

Anchorage-dependent cells are under tension that is distributed throughout the cytoskeleton; when external forces are loaded upon the cell a transient or sustained change of cellular tension occurs (13, 16). Upon exposure to frictional shear stresses, the mechanical load on endothelial cells must be absorbed by intracellular elastic elements or transmitted through the cell via rigid structures; otherwise, the cell will detach and roll with the flow. The additional stress will be concentrated wherever the cytoskeleton interacts with the plasma membrane, transmembrane proteins, and extracellular milieu (28–31). Thus, frictional shear stress communicated to the lumenal submembranous cytoskeletal structures will be transmitted to focal adhesion sites, and also to interendothelial junctions when the cells are confluent. Wang et al. (27) recently demonstrated mechanical coupling of the lumenal membrane of unsheared endothelial cells to the cytoskeleton. Actin was the primary resistance to membrane deformation (75% of total) in these experiments. The simplest interpretation of the dynamic changes of focal adhesion images reported here in relation to flow is that focal contact sites are responsive to sustained frictional shear stress, and that cytoskeletal actin is the principal transmission element.

The mechanisms of progressive alignment of focal adhesions parallel to the flow direction are unclear. Over minutes, the regions of focal contact appeared to coalesce into larger areas. Over hours, however, as revealed in time-lapse studies of the images, irregular bursts of activity for periods of several minutes at a time produced the appearance of progressive rotation of elongated areas of focal contact (e.g., Fig. 4 *b*) that eventually assumed a parallel orientation with the flow. Quantitation of remodeled areas revealed that the rates of remodeling in cells exposed to flow when compared with no-flow were not significantly different. Thus, the principal difference during flow was that the remodeling was directional. In the only other study of endothelial focal adhesion distribution in flow, Wechezak et al. (32) reported dramatic changes in focal adhesion distribution (observed before and after flow by interference reflectance microscopy) and cytoskeletal organization in subconfluent endothelial cells subjected to high shear stresses (93 dyn/cm^2). After exposure for 2 h, F-actin stress bundles and their associated focal adhesions were concentrated in the proximal cell region relative to flow direction. Although it is difficult to interpret focal adhesion dynamics from these single observations, the coincident reorganization of focal contact sites and cytoskeleton is consistent with our real-time observations and measurements in confluent cells exposed to physiological levels of shear stress (10 dyn/cm^2).

On the outside of the cell, integrins are required for attachment to extracellular adhesion proteins bound to the substratum (33, 34). Since focal adhesions first appear when the membrane–substratum distance is reduced to less than $\sim$ 50 nm, the spatial rearrangement of membrane may involve both intracellular and extracellular changes in the associations between the multiple proteins present in the focal adhesion complex. Mechanisms that drive expansion or redistribution of the focal adhesion sites include: (*a*) integrin-adhesion protein binding, (*b*) actin–linker protein association, and (*c*) linker protein–integrin association. An additional mechanism for altering membrane–substratum proximity is the clustering of integrin complexes in the plane of the membrane. In the present experiments, the principal BAEC integrin complex at focal adhesion sites was the vitronectin receptor $\alpha_v\beta_3$ (35), and the major adhesion molecule was serum vitronectin that coated the glass surface. The affinity of α-actinin for $\beta3$ integrin has not been measured. Significant binding between F-actin and α-actinin, which binds as a linker protein to β_1 integrin in chicken embryo fibroblasts, has been described (29), but other linker protein associations with integrins that have been studied to date (vinculin, talin) appear to be of low affinity.

Recently, several proteins have been identified that are tyrosine phosphorylated during cell adhesion to extracellular matrix proteins but not when the cells are attached to uncoated plastic or to polylysine (36, 37). These include pp125[FAK], a tyrosine kinase localized to focal adhesions (38), paxillin (30), and tensin and actin-binding protein (37). Inhibition of tyrosine kinase activity led to diminished phosphorylation of these proteins and inhibited the formation of focal adhesions and stress fibers (39). These studies suggest that linker protein phosphorylation on the cytoplasmic face of the plasma membrane is intimately involved in focal adhesion dynamics. It will be of interest to determine if flow can significantly affect the phosphorylation state of these proteins during the reorganization of the cytoskeleton–focal adhesion complex.

Real-time measurements in flow demonstrated only minor changes of endothelial adhesion during short and prolonged

exposure to shear stress. These data are similar to the consistent adhesion values noted in undisturbed cells during sustained nondirectional adhesion site remodeling (6). Furthermore, the rates of remodeling in flow and no-flow were similar in cells cultured on the same substratum. When the substratum was changed to denatured collagen, the remodeling rate was significantly depressed, although unaffected by flow. On a given substrate, therefore, cultured endothelial cells maintained the area of membrane–substratum interaction at a relatively constant level. This may be because of a limiting amount of organized filamentous actin in the cell. When F-actin is experimentally destabilized, focal adhesions diminished in area, cells gradually rounded up, and adhesion was eventually lost (6).

In summary, endothelial focal adhesions were revealed as surprisingly dynamic structures that undergo continuous remodeling but without a significant overall change of area of membrane contact with the substratum. In laminar flow, the remodeling became directional and focal adhesions reorganized in size and orientation, demonstrating the transcellular distribution of altered cell tension via the cytoskeleton. The implication of these observations, however, is that in addition to local effects at the lumenal cell surface, hemodynamic forces may also elicit physiological, biochemical, and gene regulatory responses at sites remote from the local region of force application. We suggest that focal adhesion sites are involved in the transmission, and possibly the transduction, of shear stress forces in the endothelium.

Acknowledgments

References

1. Verschueren, H. 1985. Interference reflection microscopy in cell biology: methodology and applications. *J. Cell Sci.* 75:279–301.

2. Gospodarowicz, D., G. Greenburg, and C. R. Birdwell. 1978. Determination of cellular shape by the extracellular matrix and its correlation with the control of cellular growth. *Cancer Res.* 38:4155–4171.

3. Burridge, K., K. Fath, T. Kelly, G. Nuckolls, and C. Turner. 1988. Focal adhesions: transmembrane junctions between the extracellular matrix and the cytoskeleton. *Annu. Rev. Cell Biol.* 4:487–525.

4. Izzard, C. S., and L. R. Lochner. 1980. Formation of cell-to-substrate contacts during fibroblast motility: an interference-reflexion study. *J. Cell Sci.* 42:81–116.

5. Paddock, S. W. 1989. Tandem scanning reflected light microscopy of cell-substratum adhesions and stress fibres in Swiss 3T3 cells. *J. Cell Sci.* 93:143–146.

6. Davies, P. F., A. Robotewskyj, and M. L. Griem. 1993. Endothelial cell adhesion in real-time. Measurements in vitro by tandem scanning confocal image analysis. *J. Clin. Invest.* 91:2640–2652.

7. Ingber, D., and J. Folkman. 1989. Mechanochemical switching between growth and differentiation during fibroblast growth factor-stimulated angiogenesis in vitro: role of extracellular matrix. *J. Cell Biol.* 109:317–330.

8. Hay, E. D., and S. Meier. 1976. Stimulation of corneal differentiation by interaction between cell surface and extracellular matrix. II. Further studies on the nature and site of transfilter "induction". *Dev. Biol.* 52:141–157.

9. Horvath, A. R., and S. Kellie. 1990. Regulation of integrin mobility and cytoskeletal association in normal and RSV-transformed chick embryo fibroblasts. *J. Cell Sci.* 97:307–315.

10. Turner, C. E., and K. Burridge. 1991. Transmembrane molecular assemblies in cell-extracellular matrix interactions. *Curr. Opin. Cell Biol.* 3:849–853.

11. Pienta, K. J., and D. S. Coffey. 1992. Nuclear-cytoskeletal interactions:

evidence for physical connections between the nucleus and cell periphery and their alteration by transformation. *J. Cell. Biochem.* 49:357–4365.

12. Dennerll, T. J., and H. C. Joshi. 1988. Tension and compression in the cytoskeleton of PC-12 neurites. II. Quantitative measurements. *J. Cell Biol.* 107:665–674.

13. Ingber, D. 1991. Integrins as mechanochemical transducers. *Curr. Opin. Cell Biol.* 3:841–848.

14. Sims, J. R., S. Karp, and D. E. Ingber. 1992. Altering the cellular mechanical force balance results in integrated changes in cell, cytoskeletal and nuclear shape. *J. Cell Sci.* 103:1215–1222.

15. Davies, P. F., and S. C. Tripathi. 1993. Mechanical stress mechanisms and the cell. An endothelial paradigm. *Circ. Res.* 72:239–245.

16. Heidemann, S. R., and R. E. Buxbaum. 1990. Tension as a regulator and integrator of axonal growth. *Cell. Motil. Cytoskeleton.* 17:6–10.

17. Welch, M. P., G. F. Odland, and R. A. Clark. 1990. Temporal relationships of F-actin bundle formation, collagen and fibronectin matrix assembly, and fibronectin receptor expression to wound contraction. *J. Cell Biol.* 110:133–145.

18. Volk, T., L. I. Fessler, and J. H. Fessler. 1990. A role for integrin in the formation of sarcomeric cytoarchitecture. *Cell.* 63:525–536.

19. Davies, P. F. 1993. Endothelium as a signal transduction interface for flow forces: cell surface dynamics. *Thromb. Haemostasis.* 70:124–128.

20. Olesen, S. P., D. E. Clapham, and P. F. Davies. 1988. Hemodynamic shear stress activates a K^+ current in vascular endothelial cells. *Nature (Lond.).* 331:168–170.

21. Prasad, A. R., S. A. Logan, R. M., C. J. Schwartz, and E. A. Sprague. 1993. Flow-related responses of intracellular inositol phosphate levels in cultured aortic endothelial cells. *Circ. Res.* 72:827–836.

22. Resnick, N., T. Collins, W. Atkinson, D. T. Bonthron, C. F. Dewey, Jr., and M. A. Gimbrone, Jr. 1993. Platelet-derived growth factor B chain promoter contains a cis-acting fluid shear-stress-responsive element. *Proc. Natl. Acad. Sci. USA.* 90:4591–4595.

23. Schwartz, S. M. 1980. Selection and characterization of bovine arterial endothelial cells. *In Vitro (Rockville).* 14:466–478.

24. Dull, R. O., J. M. Tarbell, and P. F. Davies. 1992. Mechanisms of flow-mediated signal transduction in endothelial cells: kinetics of ATP surface concentrations. *J. Vasc. Res.* 29:410–419.

25. Zand, M. S., and G. Albrecht-Buehler. 1989. Long-term observation of cultured cells by interference-reflection microscopy: near-infrared illumination and Y-contrast image processing. *Cell. Motil. Cytoskeleton.* 13:94–103.

26. Truskey, G. A., J. S. Burmeister, E. Grapa, and W. M. Reichert. 1992. Total internal reflection fluorescence microscopy (TIRFM). II. Topographical mapping of relative cell/substratum separation distances. *J. Cell Sci.* 103:491–499.

27. Wang, N., J. P. Butler, and D. E. Ingber. 1993. Mechanotransduction across the cell surface and through the cytoskeleton. *Science (Wash. DC).* 260:1124–1127.

28. Burridge, K. 1986. Substrate adhesions in normal and transformed fibroblasts: organization and regulation of cytoskeletal, membrane, and extracellular matrix components at focal contacts. *Cancer Res.* 4:18–78.

29. Otey, C. A., F. M. Pavalko, and K. Burridge. 1990. An interaction between alpha-actinin and the beta 1 integrin subunit in vitro. *J. Cell Biol.* 111:721–729.

30. Turner, C. E., J. R. Glenney, Jr., and K. Burridge. 1990. Paxillin: a new vinculin-binding protein present in focal adhesions. *J. Cell Biol.* 111:1059–1068.

31. Murphy-Ullrich, J. E., and M. Hook. 1989. Thrombospondin modulates focal adhesions in endothelial cells. *J. Cell Biol.* 109:1309–1319.

32. Wechezak, A. R., T. N. Wight, R. F. Viggers, and L. R. Sauvage. 1989. Endothelial adherence under shear stress is dependent upon microfilament reorganization. *J. Cell. Physiol.* 139:136–146.

33. Albelda, S. M., and C. A. Buck. 1990. Integrins and other cell adhesion molecules. *FASEB (Fed. Am. Soc. Exp. Biol.) J.* 4:2868–2800.

34. Charo, I. F., L. Nannizzi, J. W. Smith, and D. A. Cheresh. 1990. The vitronectin receptor alpha v beta 3 binds fibronectin and acts in concert with alpha 5 beta 1 in promoting cellular attachment and spreading on fibronectin. *J. Cell Biol.* 111:2795–2800.

35. Dejana, E., S. Colella, G. Conforti, M. Abbadini, M. Gaboli, and P. C. Marchisio. 1988. Fibronectin and vitronectin regulate the organization of their respective Arg-Gly-Asp adhesion receptors in cultured human endothelial cells. *J. Cell Biol.* 107:1215–1222.

36. Maher, P. A., E. B. Pasquale, J. Y. Wang, and S. J. Singer. 1985. Phosphotyrosine-containing proteins are concentrated in focal adhesions and intercellular junctions in normal cells. *Proc. Natl. Acad. Sci. USA.* 82:6576–6580.

37. Bockholt, S. M., and K. Burridge. 1993. Cell spreading on extracellular matrix proteins induces tyrosine phosphorylation of tensin. *J. Biol. Chem.* 268:14565–14567.

38. Schaller, M. D., C. A. Borgman, B. S. Cobb, R. R. Vines, A. B. Reynolds, and J. T. Parsons. 1992. pp125FAK a structurally distinctive protein-tyrosine kinase associated with focal adhesions. *Proc. Natl. Acad. Sci. USA.* 89:5192–5196.

39. Burridge, K., C. E. Turner, and L. H. Romer. 1992. Tyrosine phosphorylation of paxillin and pp125FAK accompanies cell adhesion to extracellular matrix: a role in cytoskeletal assembly. *J. Cell Biol.* 119:893–903.